Optimal Current Programming in Three-Phase High-Power-Factor Rectifier Based on Two Boost Converters

Predrag Pejović, *Member, IEEE,* and Žarko Janda

Abstract—Current programming in a three-phase high-power-factor rectifier based on two boost converters is discussed in this paper. It is shown that the converter currents can be expressed in terms of two mutually related auxiliary functions. The auxiliary functions are related to the input current spectrum. Optimal auxiliary functions that eliminate harmonics of the input currents are derived. A method to generate reference signals for the optimal current programming is proposed. Experimental results confirming the proposed concepts are presented.

Index Terms—AC–DC power conversion, converters, harmonic distortion, power conversion harmonics, power quality, power system harmonics, rectifiers.

I. INTRODUCTION

TO LIMIT degradation in power quality caused by nonlinear loads, several standards and recommendations were introduced and revised during the last decade. These standards require loads to draw almost sinusoidal current from the utility power network.

Efforts to maintain the power quality gained interest in three-phase harmonic-free rectification techniques. A solution to this problem, proposed in [1], applies two boost converters and a current injection device to obtain near sinusoidal input current and regulated output voltage. A quasi-resonant version of the converter [1] is presented in [2]. In [3], the converter proposed in [1] is compared to the other three-phase harmonic-free rectifiers, and it is shown that at the price of increase in the equivalent low-frequency transformer kilovoltampere rating significant savings in the switch kilovoltampere rating is achieved. Application of the method [1] in an inverter system is demonstrated in [4]. Injection of the third and sixth harmonics in order to obtain improvement in total harmonic distortions of the input currents is also discussed in [4], and an optimization is performed.

An important part of the concept is the current injection device. A special magnetic device designed for this purpose is presented in [5]. In [6] and [7], the current injection is achieved by a set of three series *L–C* branches tuned to the third harmonic of the line frequency. Drawbacks of this approach are that only the third-harmonic currents can be injected, that

the current injection network draws excessive fundamental current and increases susceptibility to resonance [8], and that the system performance is sensitive to variations of parameters in the tuned *L–C* branches [6]. Due to these drawbacks, tuned *L–C* branches seem to be abandoned in recent works.

Optimization of the injected current amplitude and phase to achieve minimum total harmonic distortion (THD) is performed in [6], and effects caused by finite-source inductance and variations of the system parameters are analyzed.

In [9] and [10], various structures of three-phase high-power-factor rectifiers are proposed, and their control is analyzed. Common to all of these structures is that they do not apply the current injection device. Instead, proposed structures apply a switching network consisting of bidirectional switches to perform a similar function. This causes the reference signals for current programming to be different from the case when the current injection device is applied. It is demonstrated that it is possible to obtain purely sinusoidal waveforms of the input currents, neglecting switching ripple, by applying current programming according to the reference signals obtained by processing of the input voltages. Control of the proposed structures is approached in time domain, analyzing the converter in subtopology intervals of 60° in phase angle.

In this paper, the converters that apply magnetic current injection device are analyzed, and the injected current spectrum is extended beyond the third harmonic in order to obtain further reduction in the input current THD. Optimization of the injected current is approached in time domain, on the waveform level, instead of the harmonic component level [4]. It is demonstrated that an ideal sinusoidal waveform of the input currents could be achieved by proper current programming in the boost converters. A method to generate reference signals for the current programming is presented and experimentally verified.

In Section II, the converter is described, and its simplified model is derived. A model of the current injection device is derived. The converter currents are discussed in Section III, and it is shown that they can be expressed in terms of two mutually related auxiliary functions defined on a 60° phase angle segment. In Section IV, optimal reference waveforms for the current programming in the boost converters are derived, providing purely sinusoidal input currents in phase with the input voltages. A method to generate the reference signals is proposed in Section V, while in Section VI the input current spectrum is related to the auxiliary functions. Experimental

results are presented in Section VII, and conclusions are given in Section VIII.

II. THE HIGH-POWER-FACTOR RECTIFIER WITH TWO BOOST CONVERTERS

The rectifier analyzed in this paper is presented in Fig. 1, and it consists of a three-phase diode bridge, two boost converters, and a current injection device.

The boost converters are applied to shape the input currents by shaping i_A and i_B and to control the output voltage. The current injection device is applied to inject the third-harmonic currents in front of the diode bridge. Its function is to divide current i_Y in three equal parts: $i_{X1} = i_{X2} = i_{X3} = i_X$, presenting a low impedance in point Y and a high impedance in the connection points to the line. There are several realizations of the current injection device: zigzag autotransformer [1]–[3], a special magnetic device [5], three series *L–C* branches with resonance tuned to the third harmonic of the line frequency [6], [7], and a wye-delta-connected transformer with unloaded delta-connected secondary [8]. In the case that an insulating transformer with a wye-connected secondary is applied at the rectifier input, a current injection device is not required, and the current injection can be performed injecting the current into the secondary neutral point [4].

To derive a model of the current injection device, let us assume that it is realized applying three single-phase transformers with wye-connected primaries and unloaded delta-connected secondaries, as depicted in Fig. 1. Assuming that magnetizing currents of the transformers are negligible, ideal transformer models can be applied. Delta-connected secondaries impose two constraints, with the first

$$(v_1 - v_Y) + (v_2 - v_Y) + (v_3 - v_Y) = 0 \qquad (1)$$

resulting in

$$v_Y = \tfrac{1}{3}(v_1 + v_2 + v_3) \qquad (2)$$

and the second that all three of the secondary currents are the same, resulting in

$$i_{X1} = i_{X2} = i_{X3} = \tfrac{1}{3}i_Y = i_X. \qquad (3)$$

Although the realization of the current injection device applying three single-phase transformers satisfies the system requirements, to obtain a cost-effective solution a three-limb core should be applied. Realization of the current injection device proposed in [5] consists of a tree-limb core and a system of three wye-connected windings having the same number of turns. The windings are arranged such that their fluxes Φ_1, Φ_2, and Φ_3 satisfy

$$\Phi_1 + \Phi_2 + \Phi_3 = 0 \qquad (4)$$

neglecting the stray flux. Differentiating (4), it can be concluded that for this realization of the current injection device (1) and (2) are satisfied. Assuming that reluctance of the core limbs is infinitely small, magnetomotive forces produced by the windings have to be equal, resulting in (3). Relaxing the assumption that the reluctance is infinitely small, the currents will contain nonzero-sequence components corresponding to
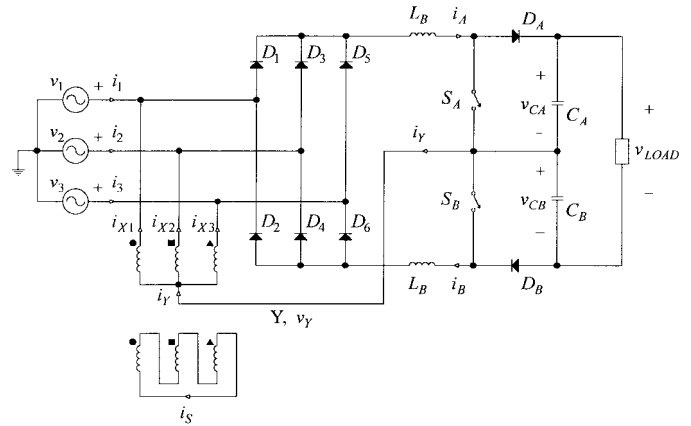

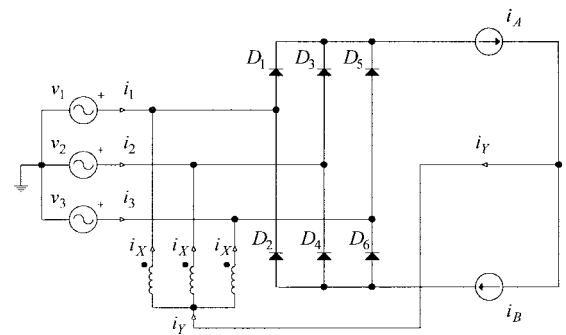Fig. 1. The high-power-factor rectifier.

Fig. 2. Simplified circuit of the rectifier.

the core magnetization. In practice, these nonzero-sequence components are very small.

Although the solution applying three-limb core and three windings is cost effective, it suffers from the influence of the stray flux on (4). To reduce the stray flux, a delta-connected secondary winding can be applied [8], or a zigzag connection of the windings [1]–[3]. Both of the techniques result in significant reduction of the stray flux, while the solution applying a zigzag connection requires less copper. In the same effort, application of an aluminum shield is described in [5].

In the analysis that follows, switching ripple in i_A and i_B is neglected, and our attention is restricted to the low-frequency part of the converter current spectra.

Under the assumptions that have been made, analysis of the input currents and their harmonic properties can be performed applying a simplified converter model presented in Fig. 2. In the model of Fig. 2, input ports of the boost converters are modeled by current sources of i_A and i_B. Currents of the sources are equal to the time average of the corresponding inductor current during the switching period.

III. ANALYSIS OF THE INPUT CURRENTS

To analyze dependence of the input current waveform on i_A and i_B, let us consider the third-harmonic injection technique applied in [1]–[7] first. According to the optimization results [6], programmed currents i_A and i_B are given by

$$i_A(\varphi) = 0.83I(1 - 0.74\sin(3\varphi)) \qquad (5)$$

and

$$i_B(\varphi) = 0.83I(1 + 0.74\sin(3\varphi)) \qquad (6)$$

where $\varphi = \omega t = 2\pi ft$ is the phase angle, f is the line frequency, and I is amplitude of the input current fundamental harmonic. Waveforms of i_A and i_B specified by (5) and (6) are presented in Fig. 3, as well as the other relevant currents of the converter.

States of the bridge diodes are determined by phase voltages v_1, v_2, and v_3, such that only one of the diodes of the group $G1 = \{D1, D3, D5\}$ and only one of the diodes of the group $G2 = \{D2, D4, D6\}$ conducts at a time point. For a specified time point, the conducting diode from the group $G1$ is a diode connected to the line with the highest of the phase voltages, while the conducting diode from the group $G2$ is a diode connected to the line with the lowest of the phase voltages.

Depending on the diode states, a line period is divided into six segments of $60°$ in phase angle, denoted by letters from A to F. Each of the time segments is defined by a pair of diodes that conduct.

Phase voltages are assumed to form a three-phase symmetrical positive-sequence voltage system

$$v_1 = V_P \sin(\varphi)$$
$$v_2 = V_P \sin(\varphi - 120°)$$
$$v_3 = V_P \sin(\varphi - 240°). \qquad (7)$$

The diode states corresponding to the phase voltages (7) are given in Table I. For convenience, the line period form $-30°$ to $330°$ in phase angle is considered.

According to the circuit diagram of Fig. 2, i_Y can be expressed as

$$i_Y = i_A - i_B \qquad (8)$$

and since that current injection device divides i_Y in three equal parts, the current injected to each phase i_X is

$$i_X = \tfrac{1}{3}i_Y = \tfrac{1}{3}(i_A - i_B). \qquad (9)$$

Waveform of the injected current is presented in Fig. 3 as well as the diode currents i_{D1} and i_{D2}.

The input currents are given by

$$i_1 = i_{D1} - i_{D2} - i_X$$
$$i_2 = i_{D3} - i_{D4} - i_X$$
$$i_3 = i_{D5} - i_{D6} - i_X. \qquad (10)$$

Waveform of the input current i_1 is presented in Fig. 3. It can be observed that the waveform is close to sinusoidal, but somewhat distorted, resulting in the power factor of PF $= 99.87\%$ and THD $= 5.125\%$. Similar diagrams can be obtained for the other two of the input currents.

In order to obtain analytical expressions for the input currents in a compact form, let us introduce two auxiliary functions $a(\varphi)$ and $b(\varphi)$ defined on a phase angle segment
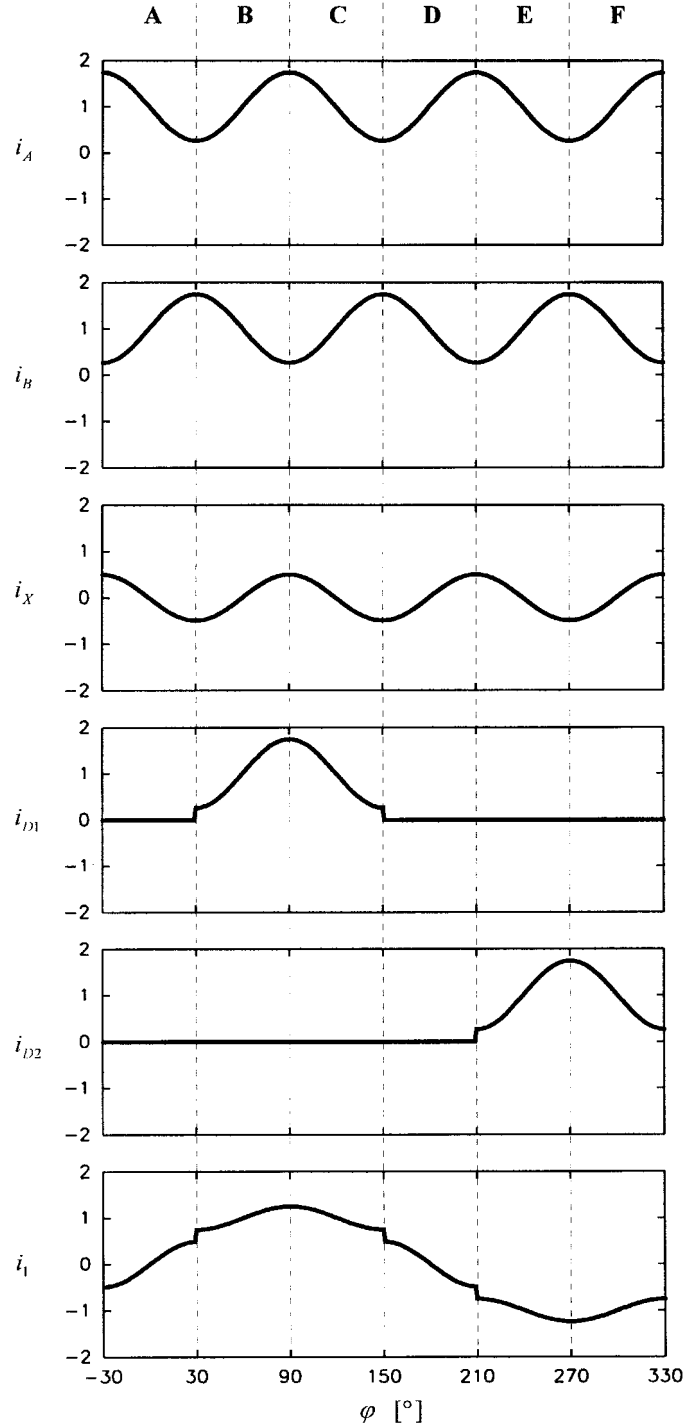

Fig. 3. Waveforms of the converter currents for the third-harmonic injection technique.

$0 \leq \varphi \leq 60°$ as

$$a(\varphi) = \frac{1}{3I}i_A(\varphi + 90°) \qquad (11)$$

and

$$b(\varphi) = \frac{1}{3I}i_B(\varphi + 90°) \qquad (12)$$

where I is amplitude of the input current fundamental harmonic.

TABLE I
CONDUCTING DIODES AND CURRENTS OF THE CONVERTER DURING THE LINE PERIOD SEGMENTS

segment	A	B	C	D	E	F
upper diode	D5	D1	D1	D3	D3	D5
lower diode	D4	D4	D6	D6	D2	D2
φ_{start}	$-30°$	$30°$	$90°$	$150°$	$210°$	$270°$
φ_{stop}	$30°$	$90°$	$150°$	$210°$	$270°$	$330°$
i_{D1}	0	i_A	i_A	0	0	0
i_{D2}	0	0	0	0	i_B	i_B
i_{D3}	0	0	0	i_A	i_A	0
i_{D4}	i_B	i_B	0	0	0	0
i_{D5}	i_A	0	0	0	0	i_A
i_{D6}	0	0	i_B	i_B	0	0
α	$\varphi+30°$	$\varphi-30°$	$\varphi-90°$	$\varphi-150°$	$\varphi-210°$	$\varphi-270°$
i_A	$3\,I\,a(\alpha)$	$3\,I\,b(\alpha)$	$3\,I\,a(\alpha)$	$3\,I\,b(\alpha)$	$3\,I\,a(\alpha)$	$3\,I\,b(\alpha)$
i_B	$3\,I\,b(\alpha)$	$3\,I\,a(\alpha)$	$3\,I\,b(\alpha)$	$3\,I\,a(\alpha)$	$3\,I\,b(\alpha)$	$3\,I\,a(\alpha)$
i_X	$I\,(a-b)$	$I\,(b-a)$	$I\,(a-b)$	$I\,(b-a)$	$I\,(a-b)$	$I\,(b-a)$
i_1	$-i_X$	i_A-i_X	i_A-i_X	$-i_X$	$-i_B-i_X$	$-i_B-i_X$
i_2	i_A-i_X	$-i_X$	$-i_B-i_X$	$-i_B-i_X$	$-i_X$	i_A-i_X
i_3	$-i_B-i_X$	$-i_B-i_X$	$-i_X$	i_A-i_X	i_A-i_X	$-i_X$
i_1/I	$-a+b$	$a+2b$	$2a+b$	$a-b$	$-a-2b$	$-2a-b$
i_2/I	$2a+b$	$a-b$	$-a-2b$	$-2a-b$	$-a+b$	$a+2b$
i_3/I	$-a-2b$	$-2a-b$	$-a+b$	$a+2b$	$2a+b$	$a-b$

In the case that the converter is operated applying the third-harmonic injection technique, the auxiliary functions are

$$a(\varphi) = 0.277(1 + 0.74\cos(3\varphi))$$
$$b(\varphi) = 0.277(1 - 0.74\cos(3\varphi)) \qquad (13)$$

as presented in Fig. 4.

Programmed currents i_A and i_B should satisfy some symmetry properties in order to obtain the input current free of even harmonics. In terms of i_A and i_B, these properties are

$$i_A(90° + \varphi) = i_A(90° - \varphi) \qquad (14)$$

and

$$i_B(\varphi) = i_A(\varphi - 60°). \qquad (15)$$

Current i_B has the same waveform as i_A, but displaced for one half of its period, which is one sixth of the line period. The symmetry constraint can be expressed in terms of the auxiliary functions as

$$a(\varphi) = b(60° - \varphi) \qquad (16)$$

which is satisfied by the auxiliary functions applied in the third-harmonic injection technique.

Expressions for i_A and i_B in terms of the auxiliary functions of the shifted argument α are given in Table I as well the expressions for α in each segment. The injected current i_X is expressed in terms of the auxiliary functions in each time segment according to (9), which is also presented in Table I. In the row where i_X is presented and below, arguments of the auxiliary functions are omitted, and it is assumed that the arguments are the same as in the expressions for i_A and i_B in the same column of the table. In the following rows of Table I, input currents are expressed in terms of i_A, i_B, and i_X in each segment, while in the last three rows input currents are expressed as linear combinations of the auxiliary functions. As expected, from the expressions in the last three rows of Table I it can be observed that i_2 and i_3 have the same waveform as i_1, but delayed in phase for $120°$ and $240°$, respectively.

IV. OPTIMAL WAVEFORM FOR THE CURRENT REFERENCE

In Section III, it is concluded that in each time point a diode from the group $G1$ connected to the line with the maximum phase voltage conducts as well as a diode from the group $G2$ connected to the line with the minimum phase voltage. Since that one phase voltage cannot be minimum and maximum at the same time, the conducting diodes are connected to different
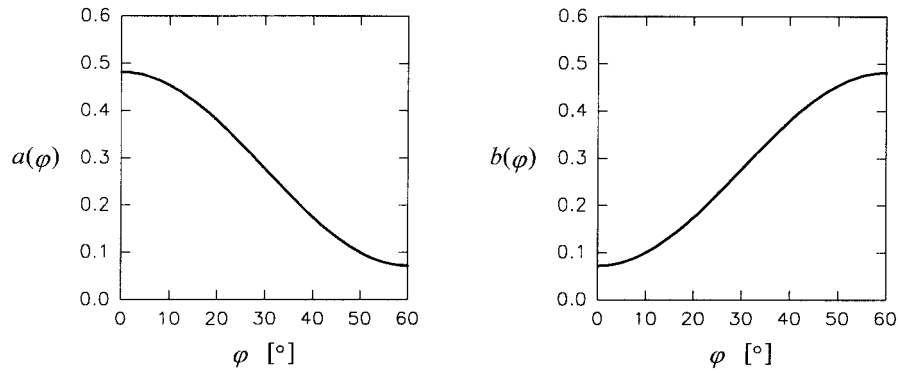
Fig. 4. Auxiliary functions for the third-harmonic injection technique.

TABLE II
GENERALIZED INPUT CURRENTS AND EXPRESSIONS FOR i_A AND i_B

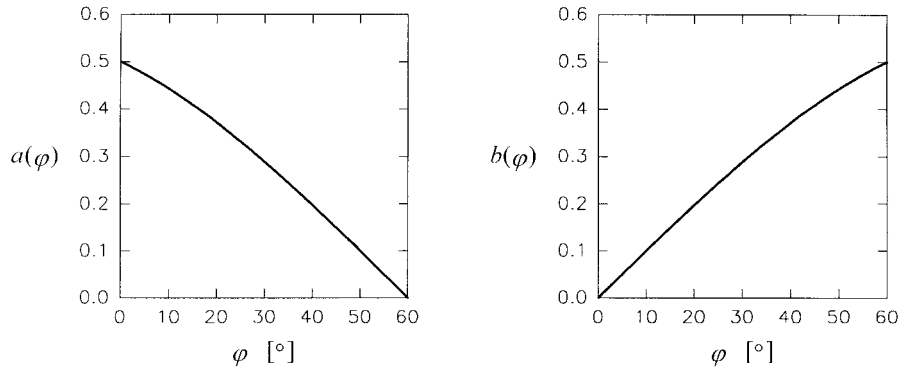| segment	A	B	C	D	E	F
i_{P1}	i_3	i_1	i_1	i_2	i_2	i_3
i_{P2}	i_2	i_2	i_3	i_3	i_1	i_1
i_{P3}	i_1	i_3	i_2	i_1	i_3	i_2
i_A	$i_3 - i_1$	$i_1 - i_3$	$i_1 - i_2$	$i_2 - i_1$	$i_2 - i_3$	$i_3 - i_2$
i_B	$i_1 - i_2$	$i_3 - i_2$	$i_2 - i_3$	$i_1 - i_3$	$i_3 - i_1$	$i_2 - i_1$

Fig. 5. Auxiliary functions for the optimal current programming.

lines. Thus, the input currents can be expressed as

$$i_{P1} = i_A - i_X \qquad (17)$$
$$i_{P2} = -i_B - i_X \qquad (18)$$

and

$$i_{P3} = -i_X \qquad (19)$$

where $P1$ is index of a line with the maximum phase voltage at the considered time point $v_{P1} = \max(v_{P1}, v_{P2}, v_{P3})$ while $P2$ is index of a line with the minimum phase voltage $v_{P2} = \min(v_{P1}, v_{P2}, v_{P3})$ at the same time point.

Equations (17)–(19) satisfy the constraint

$$i_{P1} + i_{P2} + i_{P3} = 0 \qquad (20)$$

imposed by the first Kirchhoff's law.

Within a time segment, line with the minimum and line with the maximum phase voltage remain the same. Generalized input currents i_{P1}, i_{P2}, and i_{P3} are specified in Table II.

Substituting (9) in (17)–(19), expressions for the input currents in terms of i_A and i_B are obtained as

$$i_{P1} = \tfrac{2}{3}i_A + \tfrac{1}{3}i_B \qquad (21)$$
$$i_{P2} = -\tfrac{1}{3}i_A - \tfrac{2}{3}i_B \qquad (22)$$

and

$$i_{P3} = -\tfrac{1}{3}i_A + \tfrac{1}{3}i_B. \qquad (23)$$

Since that the input currents satisfy the constraint (20), just two of them are independent. Thus, with proper current programming of i_A and i_B, it is possible to obtain arbitrary waveform of the input currents free of zero-sequence component, including purely sinusoidal.

Solving (21) and (22) over i_A and i_B

$$i_A = 2i_{P1} + i_{P2} \tag{24}$$

and

$$i_B = -i_{P1} - 2i_{P2} \tag{25}$$

is obtained. Applying constraint (20)–(24) and (25), expressions for i_A and i_B can be simplified to

$$i_A = i_{P1} - i_{P3} \tag{26}$$

and

$$i_B = i_{P3} - i_{P2}. \tag{27}$$

In Table II, expressions for i_A and i_B in terms of the input currents are given in each time segment.

Applying conditions $i_1 = I\sin\varphi$, $i_2 = I\sin(\varphi - 120°)$, and $i_3 = I\sin(\varphi - 240°)$ to the expressions for i_A and i_B given in Table II and equating the results to the corresponding expressions given in Table I, auxiliary functions are determined. For example, a system of equations over the auxiliary functions can be formed equating expressions from Table II for i_A and i_B in time segment A for input currents i_1 and i_2 to the corresponding expressions from Table I. Obtained equations are

$$3Ia(\varphi + 30°) = I\sin(\varphi - 240°) - I\sin(\varphi) \tag{28}$$

and

$$3Ib(\varphi + 30°) = I\sin(\varphi) - I\sin(\varphi - 120°). \tag{29}$$

Simplifying expressions (28) and (29), the auxiliary functions are obtained in compact form as

$$a(\varphi) = \frac{1}{\sqrt{3}}\sin(60° - \varphi) \tag{30}$$

and

$$b(\varphi) = \frac{1}{\sqrt{3}}\sin(\varphi). \tag{31}$$

The auxiliary functions specified by (30) and (31) are presented in Fig. 5.

Optimal waveforms for i_A and i_B are determined by the auxiliary functions according to the expressions given in Table I, and they are presented in Fig. 6. Period of i_A and i_B is one third of the line voltage period. Waveform of i_B is the same as of i_A, but displaced in time for one half of its period.

Proposed method of current programming result in the converter currents presented in Fig. 6. In the diagrams of Fig. 6, it can be observed that the input current i_1 is purely sinusoidal, with no distortion.

Peak values of i_A and i_B, relevant for dimensioning of the switching components, are $1.5\ I$, where I is the input current amplitude. In the case of the third-harmonic injection technique, peak values of i_A and i_B are equal to $1.444\ I$, where I is the amplitude of the input current fundamental harmonic. Thus, with negligible increase of about 4% in the switch peak
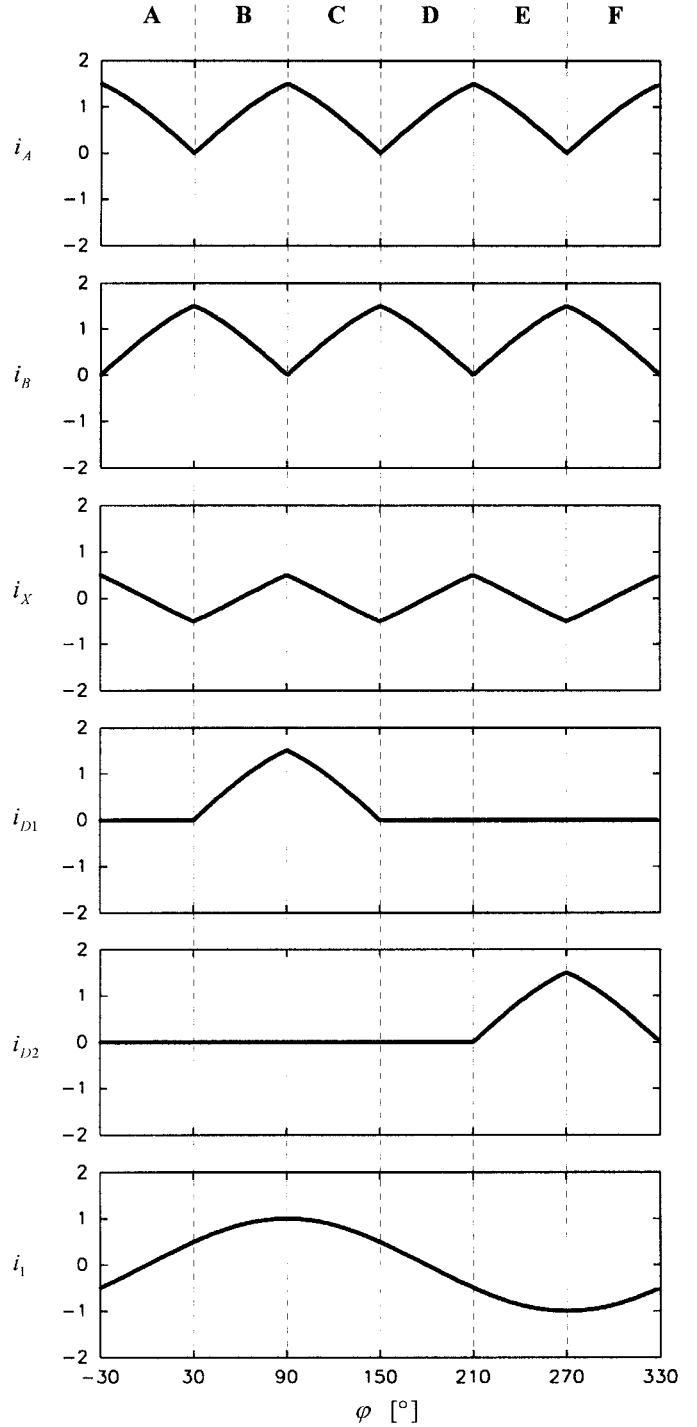

Fig. 6. Waveforms of the converter currents for the optimal current programming technique.

current, the ideal sinusoidal waveforms of the input currents are obtained.

In the waveform of the injected current i_X, it can be observed that it has discontinuous derivative that causes its spectrum, presented in Fig. 7, to contain infinite number of harmonics. Harmonic components of i_X are located at odd triples of the line frequency. The rms value of i_X, relevant for dimensioning of the current injection device, is $I_{X\,\mathrm{rms}} = 0.294\ I$ compared to $I_{X\,\mathrm{rms}} = 0.290\ I$ in the third-harmonic injection technique.
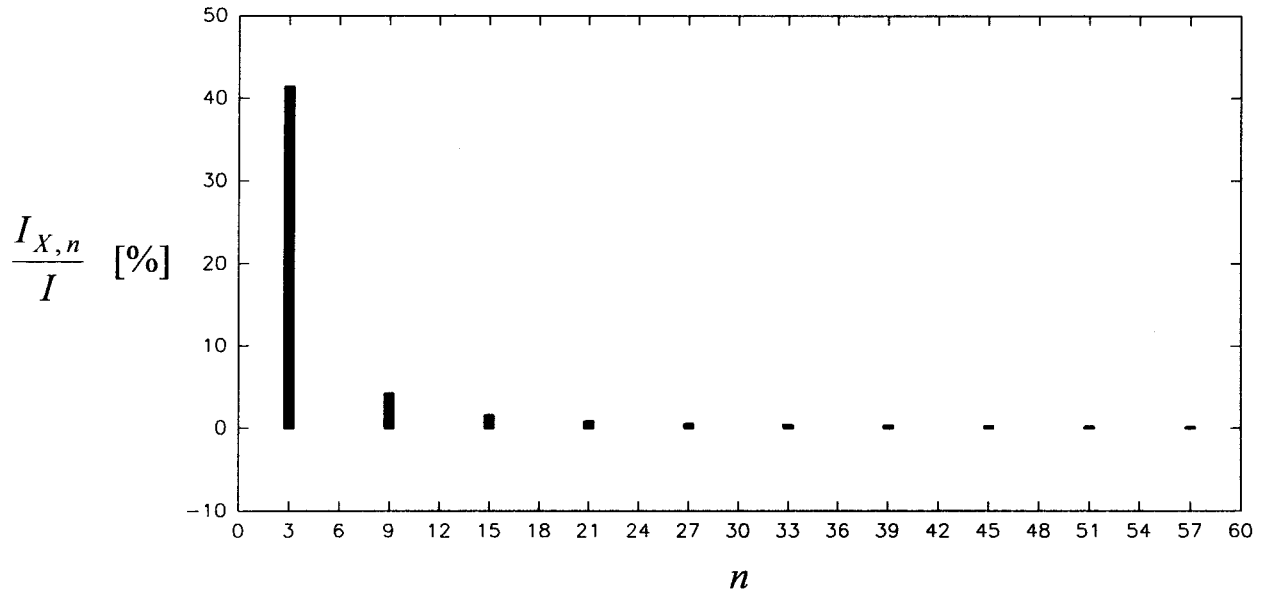
Fig. 7.   Spectrum of the injected current.

TABLE III
CURRENT REFERENCES IN TERMS OF THE LINE VOLTAGES

segment	A	B	C	D	E	F
i_A/I	v_{31}/V_P	$-v_{31}/V_P$	v_{12}/V_P	$-v_{12}/V_P$	v_{23}/V_P	$-v_{23}/V_P$
i_B/I	v_{12}/V_P	$-v_{23}/V_P$	v_{23}/V_P	$-v_{31}/V_P$	v_{31}/V_P	$-v_{12}/V_P$

V. SYNTHESIS OF THE CURRENT REFERENCE SIGNALS AND THE CONVERTER CONTROL

Control signals used as a reference for programming of i_A and i_B in the proposed method can be obtained processing the line voltages. In the text that follows, line voltages are assumed to be:

$$v_{12} = v_1 - v_2$$
$$v_{23} = v_2 - v_3 \qquad (32)$$
$$v_{31} = v_3 - v_1.$$

To obtain unity power factor the input currents should be proportional to the phase voltages

$$\frac{i_k}{I} = \frac{v_k}{V_P}, \quad \text{for } k = 1, 2, \text{ and } 3 \qquad (33)$$

where I is the amplitude of the input currents and V_P is the amplitude of the phase voltages.

According to the expressions for i_A and i_B in terms of the input currents, given in Table II, applying (33) references for the current programming of i_A and i_B are expressed in terms of the line voltages, as it is given in Table III.

From the equations of Table III, since that the reference signals for i_A and i_B are always positive, the simplest method

to generate the reference signals is switching of signals proportional to absolute values of the line voltages. To obtain proper switching, information about signs of the line voltages is required. In the equations that follow, in order to obtain compact analytical expressions, information about signs of the line voltages are obtained through the Heaviside functions of the voltages, defined as:

$$h(v) = \begin{cases} 0, & \text{for } v < 0 \\ 1, & \text{for } v \geq 0. \end{cases} \qquad (34)$$

In Fig. 8, absolute values and Heaviside functions of the line voltages, as well as required current references are presented. It can be observed that during one line period for each of the reference signals phase angle segments of $120°$ can be defined where a current reference signal has the same waveform as one of the line voltage absolute values. These segments can be determined applying simple logic operations on signals $h(v_{12})$, $h(v_{23})$, and $h(v_{31})$.

Analytically, the current reference signals according to Fig. 8 can be expressed as

$$\frac{i_A}{I} = \frac{1}{V_P}(|v_{12}|(h(v_{23})(1 - h(v_{31})))$$
$$+ |v_{23}|(h(v_{31})(1 - h(v_{12})))$$
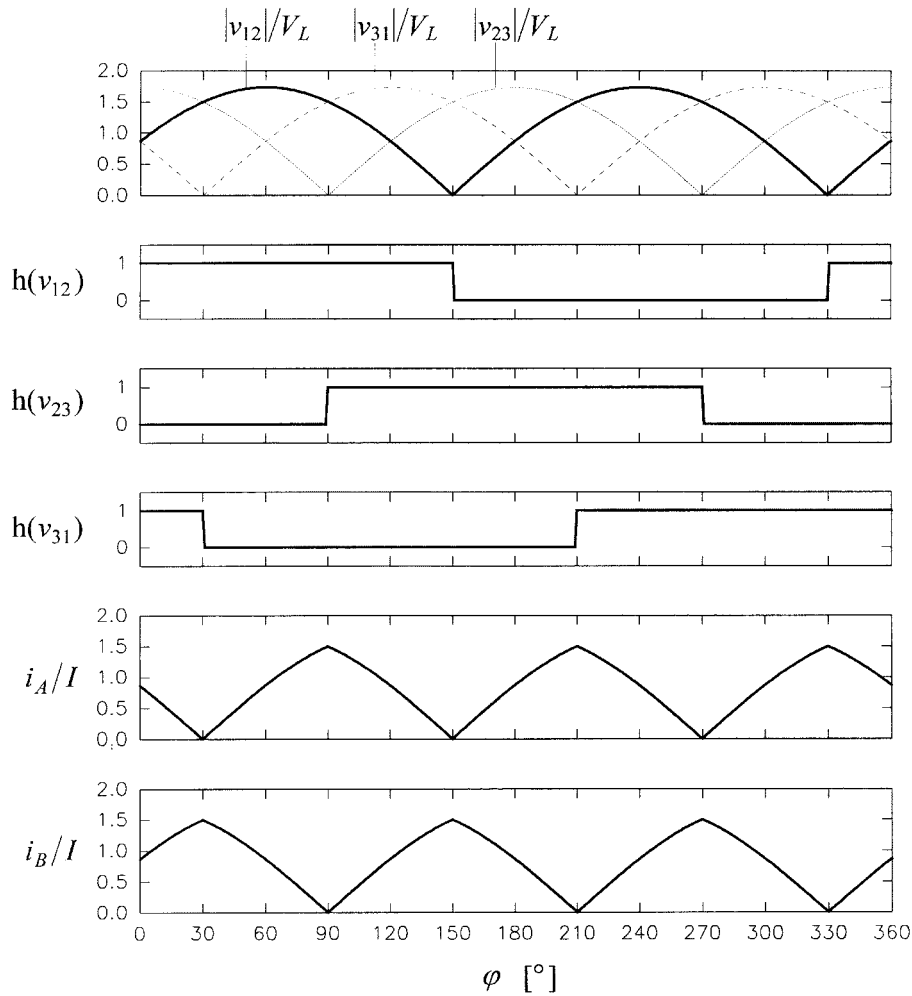$$+ |v_{31}|(h(v_{12})(1 - h(v_{23})))) \qquad (35)$$

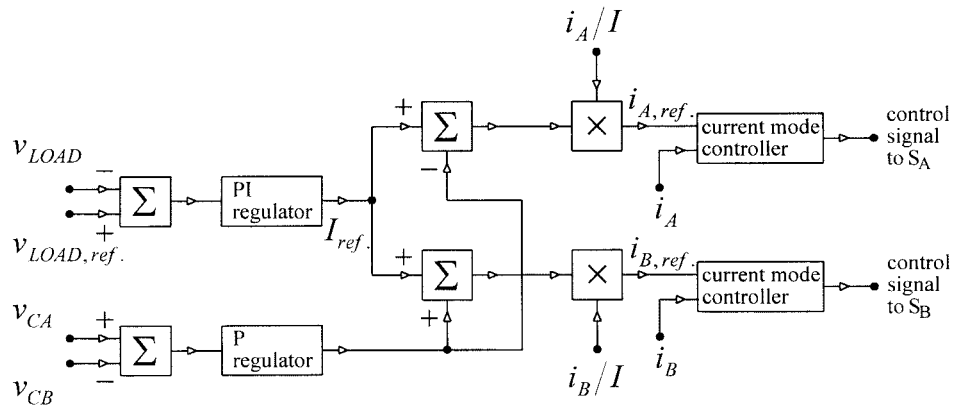Fig. 8. Absolute values and Heaviside functions of the line voltages and reference signals for i_A and i_B.

Fig. 9. Block diagram of the controller.

and

$$\frac{i_B}{I} = \frac{1}{V_P}(|v_{12}|(h(v_{31})(1 - h(v_{23})))$$

$$+ |v_{23}|(h(v_{12})(1 - h(v_{31})))$$

$$+ |v_{31}|(h(v_{23})(1 - h(v_{12})))). \qquad (36)$$

Since the arguments and the results of operations involving Heaviside functions in (35) and (36) are either zero or one, they can be realized as logic functions. Also, since the absolute values of the line voltages are multiplied either by zero or one, these operations can be realized by analog switching.

Current reference signals obtained by the proposed method are applied in a control scheme given in Fig. 9. The control scheme of Fig. 9 is based on the controller block diagram
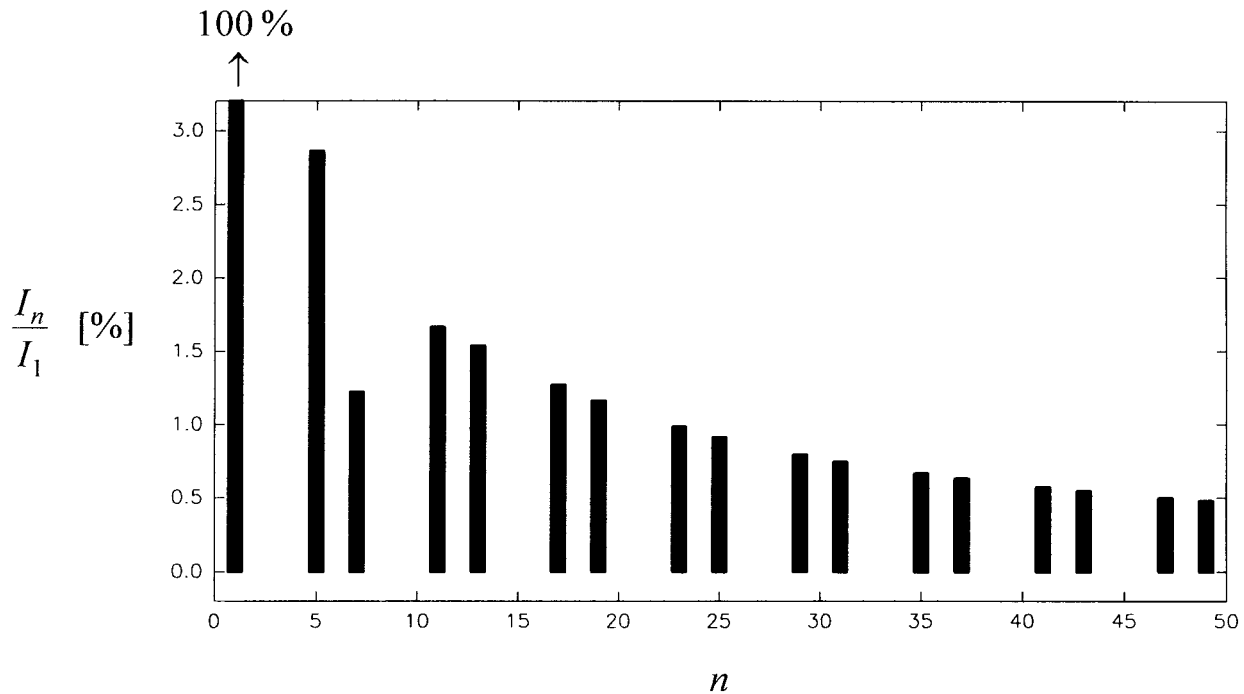
100 %

Fig. 10.   Amplitudes of the first 50 harmonics for the third-harmonic injection technique.

described in [1], and differences are caused by the different current reference. In the controller of Fig. 9, a PI regulator is applied to form a reference signal for the input current amplitude, while a P regulator is applied to equalize voltages on the output capacitors C_A and C_B. Reference signals for the current programming of i_A and i_B are obtained multiplying signals given by (35) and (36) by the input current amplitude reference. Obtained references are used to program currents i_A and i_B by average current mode controllers. Compared to the control circuit presented in [1], generation of the third-harmonic reference signal and its synchronization to the phase voltages is avoided.

The proposed method exposes distortion in the reference signals in cases that the line voltages are distorted. Experimental results illustrating this phenomenon are presented in Section VII, proving that small distortion in line voltages produces acceptable distortion in the reference signals and, thus, in the input currents. In the case that the line voltages are significantly distorted, an alternative approach based on the current reference waveforms stored in an EPROM should be applied.

VI. THE INPUT CURRENT SPECTRUM

To analyze effects of nonideal programming of i_A and i_B to the input current spectrum, the input current spectrum is related to applied auxiliary function $a(\varphi)$ in this section. It is assumed that the symmetry condition expressed by (16), which mutually relates auxiliary functions to remove even harmonics of the input currents, is satisfied. Spectrum of i_1 is considered, since that spectral content of the other two input currents is the same as for as for i_1.

The input current spectral component of order n is defined by

$$I_n = f \int_{-(1/2f)}^{1/2f} i_1(t)e^{-jn\omega t} \, dt \qquad (37)$$

where n is a whole number.

Since i_1 is an odd function $i_1(-\varphi) = -i_1(\varphi)$, and, under the symmetry constraint (16), (37) can be simplified with the integration interval reduced to one quarter of the line period. The symmetry constraint in terms of i_1 yields

$$i_1(90° - \varphi) = i_1(90° + \varphi). \qquad (38)$$

Thus, the spectrum of i_1 is determined by

$$I_n = \frac{2}{j\pi} \int_0^{\pi/2} i_1(\varphi)\sin(n\varphi) \, d\varphi \qquad (39)$$

where n is restricted to be an odd number since that the spectrum of i_1 does not contain harmonic components on even multiples of the line frequency.

Applying (39) on the analytical expressions for i_1 in segments A and B given in Table I, spectrum of the input current is obtained as

$$I_n = \frac{2}{j\pi} I \int_0^{\pi/3} a(\varphi)w(n,\varphi) \, d\varphi \qquad (40)$$

where $w(n,\varphi)$ is a weight function

$$w(\varphi,n) = \sin\left(n\frac{\pi}{6} - n\varphi\right) + \sin\left(n\frac{\pi}{6} + n\varphi\right)$$
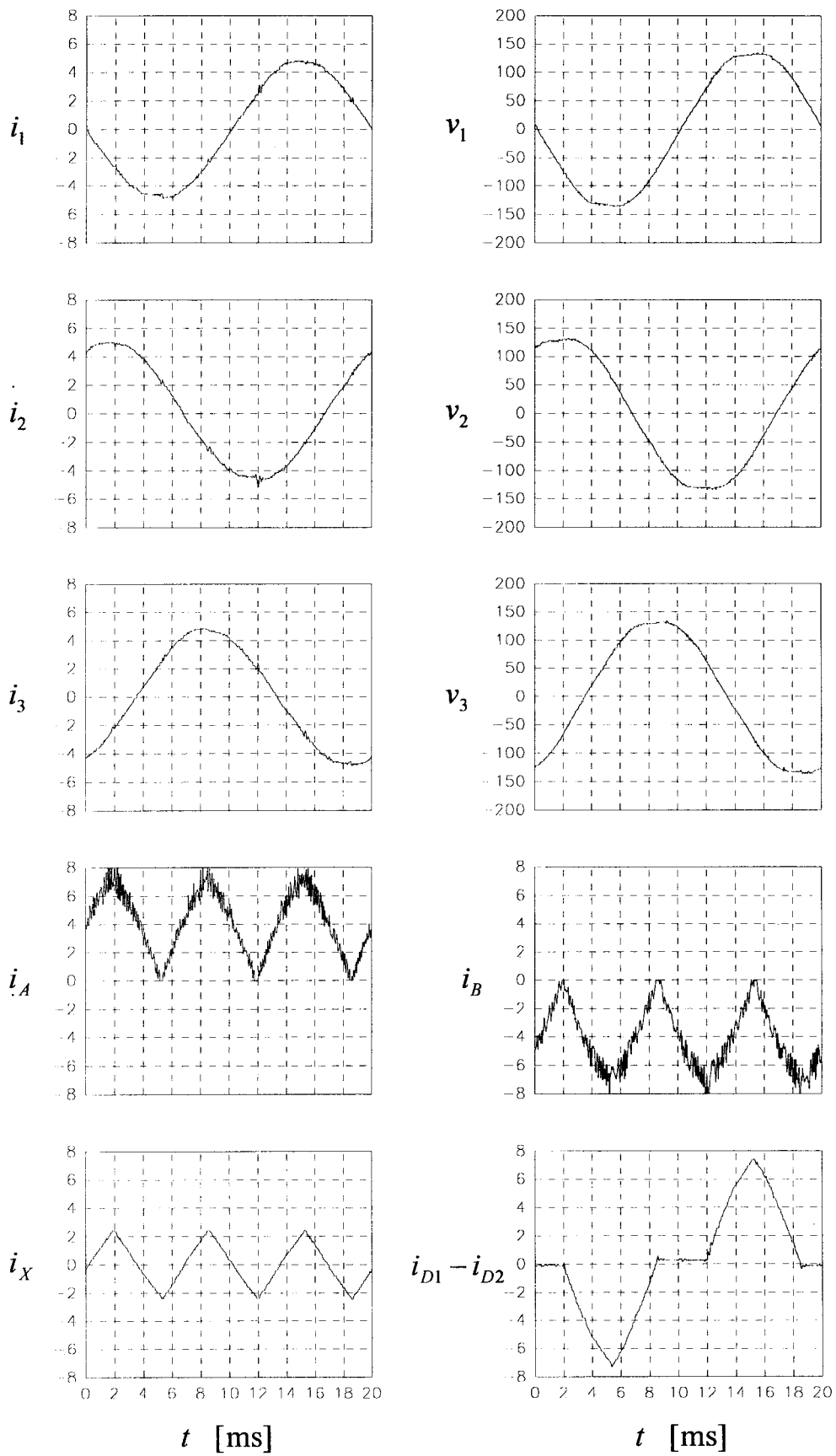$$+ 2\sin\left(n\frac{\pi}{2} - n\varphi\right). \qquad (41)$$

Fig. 11.   Experimentally obtained waveforms.

For the auxiliary function $a(\varphi)$ given by (30), in the case of optimal current programming, $I_1 = I_{-1} = (I/2)$ and $I_n = 0$ for $n \neq \pm 1$ is obtained corresponding to $i_1 = I \sin \varphi$.

Equation (40) is applied to the auxiliary function $a(\varphi)$ given by (13), proposed in the third-harmonic injection technique, in order to obtain the input current spectrum. Computation is performed applying a symbolic computation program, and amplitudes of the first 50 harmonics normalized to the fundamental harmonic are presented in Fig. 10. It can be observed that even harmonics and harmonics of the order $n = 3k$ are absent from the current spectrum. Harmonic amplitude decays slowly with the harmonic order, and a large number of harmonics have to be taken into account in order to compute THD accurately. For example, taking the first 50 harmonics into account, THD = 4.77% is obtained, while taking the first 2000 harmonics yields THD = 5.125%. Due to the presence of the current ripple, this result has primarily theoretical meaning.

VII. EXPERIMENTAL RESULTS

To verify feasibility of the proposed concept, a high-power-factor rectifier applying two boost converters is built. The converter is designed to operate at power levels up to 1.5 kW, with the rms values of the input voltages of $V_{P\,\mathrm{rms}} = 100$ V and the output voltage of $V_{\mathrm{OUT}} = 400$ V. The current mode control is implemented applying hysteresis band control with the hysteresis window of $\Delta i_L = 1.25$ A, resulting in the maximum switching frequency of $f_{S\,\max} \cong 20$ kHz for the inductors of $L - 2$ mH. To remove ripple from the input currents, capacitors of $C_F = 4.7\,\mu$F at the ac side of the diode bridge are applied. The current injection is performed by a current injection device based on a three-limb core with zigzag interconnected windings.

Experimentally obtained waveforms of the converter voltages and currents corresponding to the power level of $P = 1100$ W are presented in Fig. 11. The waveforms are recorded applying a digital oscilloscope operating in the sample acquisition mode.

Waveforms of the phase voltages provided by the utility distribution network are somewhat distorted, resulting in THD values presented in Table IV. This distortion causes some distortion of the current reference signals and, thus, in the input currents. THD values of the input currents are somewhat higher than the THD values of the input voltages, which is primarily caused by the remaining switching ripple in the waveforms. Each THD value presented in Table IV is computed from the first 250 harmonics of the waveform, obtained applying the discrete Fourier transform over 500 samples provided by the oscilloscope. Reducing attention in the THD computations to the first 50 harmonics, THD values of the input voltages and currents of about 2.5% are obtained, leading to the conclusion that the difference between the input voltage THD and the input current THD is primarily caused by the switching ripple.

Waveforms of i_A and i_B are recorded before the filtering, and the switching ripple can be observed, while the other currents are recorded after the filtering, resulting in the significantly reduced switching ripple.

TABLE IV
DISTORTIONS OF THE INPUT VOLTAGES AND CURRENTS

j	$THD(v_j)$	$THD(i_j)$
1	2.89 %	3.49 %
2	2.47 %	3.17 %
3	2.78 %	3.10 %

The waveforms presented in Fig. 11 agree with the theoretical predictions.

VIII. CONCLUSIONS

Current programming in three-phase high-power-factor rectifier based on two boost converters is discussed in the paper. The converter provides high-power-factor, regulated output voltage, and unidirectional power flow.

It is shown that the converter currents can be expressed in terms of two mutually related auxiliary functions defined on phase angle interval of $60°$. The auxiliary functions are related to the input current spectrum. Optimal auxiliary functions that eliminate harmonics of the input currents are derived. It is shown that ideal sinusoidal input currents can be obtained on the price of increase in the switch peak current of just 4% compared to the third-harmonic injection technique. Spectrum of the injected current is presented, and it is shown that it contains components on odd triples of the line frequency.

A method to generate reference signals for the optimal current programming on the basis of the line voltages is proposed. The method yields simple control circuitry.

Experimental results confirming the proposed concepts are presented.

REFERENCES

[1] R. Naik, M. Rastogi, and N. Mohan, "Third-harmonic modulated power electronics interface with three-phase utility to provide a regulated dc output and to minimize line-current harmonics," *IEEE Trans. Ind. Applicat.*, vol. 31, no. 3, pp. 598–601, 1995.

[2] M. Rastogi, N. Mohan, and C. Henze, "Three-phase sinusoidal current rectifier with zero-current switching," *IEEE Trans. Power Electron.*, vol. 10, no. 6, pp. 753–759, 1995.

[3] M. Rastogi, R. Naik, and N. Mohan, "A comparative evaluation of harmonic reduction techniques in three-phase utility interface of power electronic loads," *IEEE Trans. Ind. Applicat.*, vol. 30, no. 5, pp. 1149–1155, 1994.

[4] R. Naik, N. Mohan, M. Rogers, and A. Bulawka, "A novel grid interface, optimized for utility-scale applications of photovoltaic, wind-electric, and fuel-cell systems," *IEEE Trans. Power Delivery*, vol. 10, no. 4, pp. 1920–1926, 1995.

[5] R. Naik, M. Rastogi, N. Mohan, R. Nilssen, and C. Henze, "A magnetic device for current injection in a three-phase, sinusoidal-current utility interface," in *IEEE/IAS Annu. Meeting*, 1993, pp. 926–930.

[6] M. Rastogi, R. Naik, and N. Mohan, "Optimization of a novel dc-link current modulated interface with 3-phase utility systems to minimize line current harmonics," in *IEEE PESC*, 1992, pp. 162–167.

[7] N. Mohan, M. Rastogi, and R. Naik, "Analysis of a new power electronics interface with approximately sinusoidal 3-phase utility currents and a regulated dc output," *IEEE Trans. Power Delivery*, vol. 8, no. 2, pp. 540–546, 1993.

[8] S. Kim, P. Enjeti, P. Packebush, and I. Pitel, "A new approach to improve power factor and reduce harmonics in a three-phase diode rectifier type utility interface," *IEEE Trans. Ind. Applicat.*, vol. 30, no. 6, pp. 1557–1564, 1994.

[9] J. Salmon, "Operating a three-phase diode rectifier with a low-input current distortion using a series-connected dual boost converter," *IEEE Trans. Power Electron.*, vol. 11, no. 4, pp. 592–603, 1996.

[10] ———, "Reliable 3-phase PWM boost rectifiers employing a stacked dual boost converter subtopology," *IEEE Trans. Ind. Applicat.*, vol. 32, no. 3, pp. 542–551, 1996.

Predrag Pejović (SM'91–M'96) was born in 1966 in Belgrade, Yugoslavia. He received the B.S. and M.S. degrees in electrical engineering from the University of Belgrade, Belgrade, and the Ph.D. degree from the University of Colorado, Boulder, in 1990, 1992, and 1995, respectively.

Since 1995, he has been an Assistant Professor at the University of Belgrade. His current research interests include three-phase low-harmonic rectifiers, electronic measurements, and techniques for computer-aided analysis and design of power electronic systems.

Žarko Janda was born in 1960 in Čačak, Yugoslavia. He received the B.S. and M.S. degrees in electrical engineering from the University of Belgrade, Belgrade, Yugoslavia, in 1984 and 1989, respectively. He is currently working towards the Ph.D. degree in the area of high-power-factor rectifiers at the University of Belgrade.

Since 1984, he has been with the Department of Control, Institute Nikola Tesla, Belgrade, where he works on high-power converters, uninterruptible power supplies, and adjustable-speed drives as a Leading Engineer. From 1990 to 1991, he was a Visiting Student at Concordia University, Montreal, Canada. His research interests include high-power-factor rectifiers, uninterruptible power supplies, and adjustable-speed drives.